

## Enhanced absorption Hanle effect in the configuration of crossed laser beam and magnetic field

F. Renzoni,<sup>1,\*</sup> S. Cartaleva,<sup>2,†</sup> G. Alzetta,<sup>2</sup> and E. Arimondo<sup>2</sup>

<sup>1</sup>*Institut für Laser-Physik, Universität Hamburg, Jungiusstrasse 9, D-20355 Hamburg, Germany*

<sup>2</sup>*Istituto Nazionale per la Fisica della Materia and Dipartimento di Fisica, Università di Pisa, I-56126 Pisa, Italy*

(Received 16 November 2000; published 10 May 2001)

We have analyzed the Hanle effect on the closed  $F_g=3 \rightarrow F_e=4$   $D_2$ -line transition of  $^{85}\text{Rb}$ . Exciting the rubidium atoms by circularly polarized laser light, and scanning an applied transverse magnetic field, a bright resonance Hanle signal is obtained at different values of an applied longitudinal magnetic field. We report experimental and numerical evidence of this bright resonance.

DOI: 10.1103/PhysRevA.63.065401

PACS number(s): 32.80.Bx, 32.80.Qk

In a multilevel atomic system the creation of low-frequency coherences, and eventually their circulation through absorption and spontaneous emission processes, leads to significant modifications of the atomic fluorescence line shape. Well-known examples of these modifications are the Hanle effect [1] and coherent population trapping [2]. Low-frequency coherences also lead to drastic modifications of the absorptive and dispersive properties of atomic media [2–4], and are responsible for the sub-Doppler [5,6] and sub-recoil [7] temperatures reached in the laser cooling processes with counterpropagating  $\sigma^+$  and  $\sigma^-$  laser fields. Recently an investigation of a multilevel atomic system with two optical fields revealed that the combined actions of the two coherent optical fields produces a low-frequency Zeeman coherence that increases the atomic absorption [8,9]. The increased atomic absorption, denoted as electromagnetic induced absorption or bright resonance, was observed by scanning the frequency difference between the two optical fields creating the low-frequency coherence.

The production and destruction of low-frequency coherences can also be properly studied in the Hanle configuration with a single laser field applied to an atomic transition, and the Zeeman degeneracy in the lower and upper states broken by an applied magnetic field. It should be noted that similar experimental configurations, and theoretical approaches, apply to Hanle effect dark-state and bright resonances. While the Hanle configuration for the dark-state coherences was studied in Ref. [10], that for the bright resonances was recently investigated experimentally in Ref. [11], with a theoretical analysis in Ref. [12]. Bright resonances appear as an increased atomic fluorescence, following laser excitation on the  $F_g \rightarrow F_e = F_g + 1$  transition. The bright resonance Hanle effect is based on the laser creation of large Zeeman ground-state coherences at zero magnetic field, and their destruction at nonzero values of the magnetic field. Equivalently, in a rotated atomic basis, the effect is associated with the optical pumping, at zero magnetic field, of the atomic population in the ground-state sublevels maximally excited by laser fields,

and with the destruction of the population difference through the magnetic-field-created Zeeman coherences.

The Hanle effect investigations of Refs. [11,12] were based on a linearly polarized laser field and a magnetic field parallel to the light propagation direction. However, in this configuration the measured fluorescence increases, due to the low-frequency coherence, are very modest, of the order of 1% of the broad fluorescence background. In the present work we theoretically and experimentally demonstrate the effect of enhanced absorption in a different ground-state Hanle effect configuration. In this configuration, a circularly polarized laser field excites the closed  $F_g = F \rightarrow F_e = F + 1$  transition, and a transverse magnetic field, applied orthogonally to the light propagation direction, is scanned around zero. It will be shown that for this configuration the bright resonance fluorescence increase is more pronounced than for the previous configuration. The larger atomic coherences will allow applications of bright resonances to quantum optics and nonlinear wave mixing. We also examine, both experimentally and theoretically, the influence of ground-state relaxations and spurious magnetic fields on the bright resonance strength.

In the experiment  $^{85}\text{Rb}$  vapor, contained in a vacuum cell, was excited by circularly polarized light in resonance with the transition  $F_g=3 \rightarrow F_e=4$  of the  $D_2$  line. Owing to the atomic Doppler distribution, the laser light excited several hyperfine transitions of the  $D_2$  line. However, because the closed  $F_g=3 \rightarrow F_e=4$  transition is the strongest hyperfine transition with efficient optical pumping, the largest contribution to the atomic fluorescence arises from this transition. Magnetic fields  $B_z$  along the  $Oz$  axis of the laser propagation direction and  $B_x$  along the  $Ox$  orthogonal direction were applied, or scanned around the zero value. Additional coils compensated for the external magnetic fields within a 50-mG range. The atomic fluorescence was monitored while scanning the  $B_x$  field.

Figure 1 shows experimental results for the emitted atomic fluorescence in the present bright resonance configuration, with circularly polarized laser light and the  $B_x$  magnetic field scanned around zero for different values of the applied static magnetic field  $B_z$  along the  $Oz$  axis. Only the narrow central part of the Hanle resonance, with a linewidth around 30 mG, is shown in the figure. This narrow resonance is superimposed on the broader structure associated with the inhomogeneous linewidth of the optical transition.

\*Present address: Laboratoire Kastler-Brossel, Département de Physique de l'École Normale Supérieure, 24 rue Lhomond, 75231 Paris Cedex 05 France.

†Permanent address: Institute of Electronics, Bulgarian Academy of Sciences, Boul. Tsarigradsko Shosse 72, 1784 Sofia, Bulgaria.

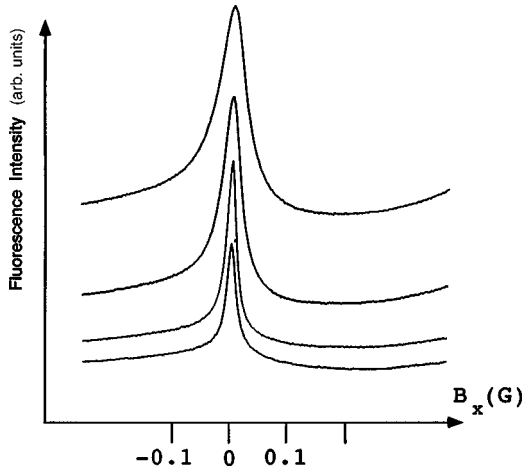


FIG. 1. Experimental results for the fluorescence emitted from a  $^{85}\text{Rb}$  vapor excited with a circularly polarized laser field on the  $F_g = 3 \rightarrow F_e = 4$   $D_2$ -line transition while scanning the magnetic field  $B_x$ , at different values of  $B_z$ : 0, 0.37, 0.73, and 1.09 G, respectively, starting from the bottom curve. The laser intensity was  $3.2 \text{ mW/cm}^2$ . The zero level of the atomic fluorescence, far below the bottom horizontal line, was shifted up on the vertical scale increasing  $B_z$ .

The amplitude of the bright resonance depends on the value of the magnetic field applied along the  $Oz$  axis, with the maximum value detected at an applied  $B_z$  value around 0.25 G. The amplitude of the bright resonance was characterized through the contrast  $R$ , defined as the ratio between the intensity of the narrow fluorescence structure and the intensity of the broad background fluorescence. Experimental results for  $R$  versus the applied  $B_z$  magnetic field are shown in Fig. 2 at different laser intensities. The good ( $+B_z, -B_z$ ) symmetry of the data of Fig. 2 demonstrate the good alignment of  $B_z$  with the light propagation direction. Values of  $R$  up to 30% have been measured, to be compared with measurements for  $R$  of the order of 1% for the  $(\text{lin}, \vec{k} \parallel \vec{B})$  configuration, as reported in Ref. [11].

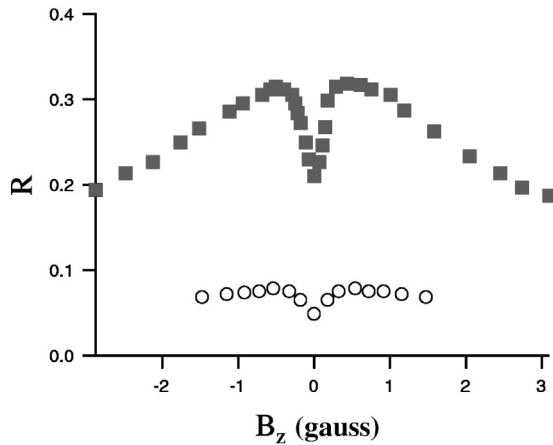


FIG. 2. Experimental data for the bright line ratio  $R$  in the experimental conditions of Fig. 1, vs the static applied  $B_z$  field, with laser light intensities of  $3.2 \text{ mW cm}^{-2}$  (squares), and  $0.32 \text{ mW cm}^{-2}$  (circles).

The experimental data have been analyzed through optical Bloch equations (OBE's) for  $^{85}\text{Rb}$  illuminated by a  $\sigma^+$  laser field propagating along the  $Oz$  axis and resonant with the  $F_g = 3 \rightarrow F_e = 4$   $D_2$ -line transition, in the presence of magnetic fields along different axes. The analysis follows the previous OBE solution applied for the dark resonances, except for additional terms produced by the presence of transverse magnetic fields [10].

Choosing the  $z$  propagation axis as the quantization axis, the OBE's for a closed transition have the following forms ( $|e_j\rangle = |J_e, I, F, j\rangle, |g_j\rangle = |J_g, I, F_g, j\rangle$ ):

$$\dot{\rho}_{e_i e_j} = -[i\omega_{e_i e_j} + \Gamma]\rho_{e_i e_j} + \frac{i}{\hbar} \sum_{g_k} (\rho_{e_i g_k} V_{g_k e_j} - V_{e_i g_k} \rho_{g_k e_j}), \quad (1a)$$

$$\dot{\rho}_{e_i g_j} = -\left[i\omega_{e_i g_j} + \frac{\Gamma}{2}\right]\rho_{e_i g_j} + \frac{i}{\hbar} \left( \sum_{e_k} \rho_{e_i e_k} V_{e_k g_j} - \sum_{g_k} V_{e_i g_k} \rho_{g_k g_j} \right), \quad (1b)$$

$$\dot{\rho}_{g_i g_j} = -i\omega_{g_i g_j} \rho_{g_i g_j} + \frac{i}{\hbar} \sum_{e_k} (\rho_{g_i e_k} V_{e_k g_j} - V_{g_i e_k} \rho_{e_k g_j}) + \left( \frac{d}{dt} \rho_{g_i g_j} \right)_{SE}. \quad (1c)$$

Here  $\Gamma$  is the spontaneous emission rate for any excited level, and  $V_{e_k, g_j}$  the matrix element of the atom-laser interaction Hamiltonian in the dipole and rotating-wave approximations. The quantities  $\omega_{\alpha_i, \beta_j}$  represent the frequency separation between the energies of levels  $\alpha_i$  and  $\beta_j$ , including the Zeeman splitting  $g_\alpha \mu_B m_i B_z$  due to the  $B_z$  magnetic field. Here  $\mu_B$  is the Bohr magneton, and  $g_\alpha$ , with  $\alpha, \beta = (e, g)$ , the gyromagnetic factor of the ground or excited state. In Eq. (1c) SE indicates the spontaneous emission repopulation terms for the density matrix evolution (see Ref. [6] for their explicit form). A transverse magnetic field, for instance  $B_x$  along the  $Ox$  axis, results in additional terms in the density-matrix equations

$$\dot{\rho}_{e_i e_j}|_{B_x} = -i \frac{\mu_B B_x}{2\hbar} g_e \{ c_{ei}^+ \rho_{e_{i+1}, e_j} + c_{ei}^- \rho_{e_{i-1}, e_j} - c_{ej}^+ \rho_{e_i, e_{j+1}} - c_{ej}^- \rho_{e_i, e_{j-1}} \}, \quad (2a)$$

$$\dot{\rho}_{e_i g_j}|_{B_x} = -i \frac{\mu_B B_x}{2\hbar} \{ g_e [ c_{ei}^+ \rho_{e_{i+1}, g_j} + c_{ei}^- \rho_{e_{i-1}, g_j} ] - g_g [ c_{gj}^+ \rho_{e_i, g_{j+1}} + c_{gj}^- \rho_{e_i, g_{j-1}} ] \}, \quad (2b)$$

$$\dot{\rho}_{g_i g_j}|_{B_x} = -i \frac{\mu_B B_x}{2\hbar} g_g \{ c_{gi}^+ \rho_{g_{i+1}, g_j} + c_{gi}^- \rho_{g_{i-1}, g_j} - c_{gj}^+ \rho_{g_i, g_{j+1}} - c_{gj}^- \rho_{g_i, g_{j-1}} \}, \quad (2c)$$

where

$$c_{FM}^{\pm} \equiv \sqrt{(F \mp M)(F \pm M + 1)}, \quad (3)$$

and we abbreviated the subscript  $F_{\alpha}$  by  $\alpha$  ( $\alpha = e, g$ ).

For the OBE solution we assumed the laser light to be near resonant with the  $^{85}\text{Rb}$   $F_g = 3 \rightarrow F_e = 4$  atomic hyperfine transition, and supposed only a natural broadening of the optical transition, as for a cold atomic sample. Moreover, for a cold sample the interaction time between the laser and atoms may be assumed to be long enough for us to consider only a steady-state solution of the density-matrix equations. In the experimental results of the present work, the bright line was detected as an increase of the fluorescence intensity. For a laser-excited closed transition, the atoms reach a steady state, and the fluorescence intensity emitted from the cold atomic sample interacting with the laser beam is proportional to the total steady-state population of the excited state,  $\Pi_{st}^e$ . Thus the dependence of this quantity on the amplitude of the applied magnetic field produces the Hanle effect line shapes observed on the fluorescence emission.

Reference [13], examining the role of Doppler broadening on coherent population trapping, showed that the Doppler broadening associated with the optical transition has a negligible influence on the measured contrast and width of the dark resonance. We have verified through numerical calculations that this is also true for the bright resonance, and therefore we have not included Doppler broadening in most analyses. Finally, due to Doppler broadening and the finite interaction time, the laser intensities needed to saturate an atomic vapor are much larger than for a cold sample [14]. Therefore, we expect that the effects observed in an atomic vapor at a given laser intensity will be reproduced by our numerical calculations on cold atoms at a much lower intensity of the laser fields.

We solved the OBE for the  $(\sigma^+, \vec{k} \perp \vec{B})$  configuration experimentally investigated in the present work, with a transverse magnetic field  $B_x$  scanned around zero. Results for the total population of the excited state  $\Pi_{st}^e$  as a function of the applied magnetic field  $B_x$  are shown in Fig. 3 for different laser intensities. A subnatural bright resonance appears superimposed on a broad profile. In fact, in the absence of a transverse magnetic field, the  $\sigma^+$ -polarized laser light pumps all the atomic population on the  $|F_g = 3, M_F = 3\rangle \leftrightarrow |F_e = 4, M_F = 4\rangle$  Zeeman transition, which is the strongest one. The application of a transverse magnetic field, producing low-frequency coherences between the ground Zeeman sublevels, redistributes the population among the Zeeman sublevels, with a decrease of the fluorescence intensity.

Our numerical calculations confirm that the effect of bright resonances is much more pronounced for the configuration of crossed laser beam and magnetic field  $(\sigma^+, \vec{k} \perp \vec{B})$  examined in this work than for the configuration  $(\text{lin}, \vec{k} \parallel \vec{B})$  considered in Refs. [11,12]. The numerically calculated amplitude of the  $(\text{lin}, \vec{k} \parallel \vec{B})$  bright resonance is in fact about one-tenth of the broad fluorescence signal [12], to be compared with the  $(\sigma^+, \vec{k} \perp \vec{B})$  configuration investigated in Fig. 3, for which the amplitude of the bright resonance has about the same amplitude as the broad structure.

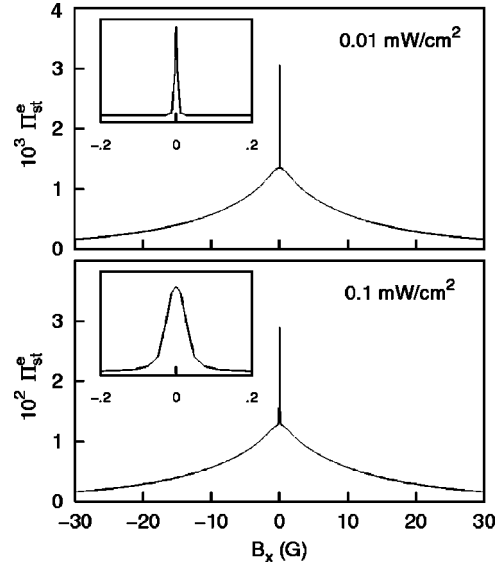


FIG. 3. Numerical results for the  $F_g = 3 \rightarrow F_e = 4$   $^{85}\text{Rb}$   $D_2$ -line bright resonance in the  $(\sigma^+, \vec{k} \perp \vec{B})$  configuration. The steady-state total population of the excited state, as a function of the  $B_x$  field for different laser intensities, is at  $B_z = 0$ . The insets show the regions around zero magnetic field.

The predicted ratio  $R$  between the amplitude of the narrow resonance and the broad profile of Fig. 3 is nearly constant over the examined range of laser intensities. By contrast, in the experimental results  $R$  increases with the laser intensity. This different behavior can be explained by the presence of relaxation processes in the ground state. In this case an efficient optical pumping is obtained for a pumping rate  $\Omega^2/\Gamma$  larger than the ground-state relaxation rate  $\gamma$ , and the ratio  $R$  becomes, for weak laser fields, an increasing function of the laser intensity via  $\Omega^2/\Gamma \gamma$ . A finite interaction time  $\theta$ , corresponding to a relaxation rate  $\gamma = 1/\theta$ , and the additional transverse stray fields, to be included in the following analysis, are equivalent to ground-state relaxation processes. We have verified numerically that the ground-state relaxation processes modify the dependence of  $R$  on the laser intensity, but a fit of the experimental results cannot be performed without a characterization of the relaxation processes.

In order to analyze the experimental results of Fig. 1 for the dependence of the ratio  $R$  on the longitudinal applied  $B_z$  magnetic field, we have theoretically examined the effect of a longitudinal magnetic field  $B_z$  on the bright resonance. Numerical results for the bright resonance, scanning the  $B_x$  field, supposing  $B_y = 0$ , and at different values of the longitudinal  $B_z$  magnetic field, showed a contrast of the bright resonance slightly decreasing with increasing strength of the  $B_z$  magnetic field, in contrast with the experimental observations of Fig. 2. The presence of laser detunings did not modify this result. However, in the presence of stray magnetic fields, the application of a  $B_z$  field different from zero should help the optical pumping by the  $\sigma^+$ -polarized light. Thus, we included in our numerical analysis a weak magnetic field  $B_y$  along the  $y$  axis. Results for the excited-state population as a function of the scanning magnetic field  $B_x$  at

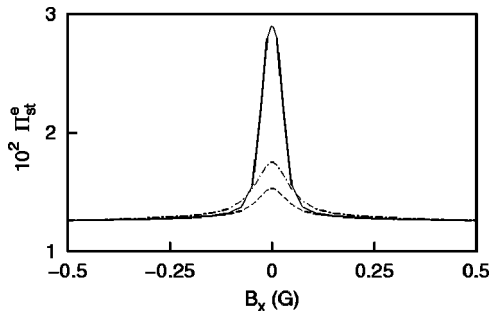


FIG. 4. Numerical results for the  $F_g=3 \rightarrow F_e=4$   $^{85}\text{Rb}$   $D_2$ -line bright resonance in the  $(\sigma^+, \vec{k} \perp \vec{B})$  configuration, at a laser intensity of  $0.1 \text{ mW/cm}^2$ . The steady-state total population of the excited state as a function of the applied  $B_x$  magnetic field for different values of  $B_y$  and  $B_z$ . Continuous line:  $B_z=B_y=0$ . Dashed line:  $B_z=0$  and  $B_y=50 \text{ mG}$ . Dot-dashed line:  $B_z=20 \text{ mG}$  and  $B_y=50 \text{ mG}$ . Only the region around zero magnetic field is shown.

different values of the ‘‘stray’’ magnetic field  $B_y$  are shown in Fig. 4. It appears that, at  $B_z=0$ , the presence of the stray magnetic field  $B_y$  leads to a drastic reduction of the amplitude of the bright resonance with respect to the ideal case  $B_y=0$  previously analyzed. The stray magnetic field  $B_y$ , mixing the Zeeman sublevels, produces a disturbance of the  $\sigma^+$  optical pumping. The application of a longitudinal magnetic field  $B_z$  restores the  $\sigma^+$  optical pumping, and therefore leads to an increase in the amplitude of the bright resonance. Thus the experimental results of Fig. 2 are associated with the presence of an additional transverse magnetic field in the 50-mG range.

As an additional test of the role of the stray magnetic fields, we calculated, at different laser intensities, the ratio  $R$  for a bright resonance in the  $(\sigma^+, \vec{k} \perp \vec{B})$  configuration as a function of the longitudinal magnetic field  $B_z$  in the presence of a stray magnetic field  $B_y=10 \text{ mG}$ . The numerical results demonstrate that the residual magnetic field along the  $Oy$  axis indeed introduces an increasing dependence of  $R$  on the laser intensity, for a small  $B_z$  field. However, we could not reproduce the decrease of Fig. 2 at a larger magnetic field  $B_z$ , proving that a better control of the experimental conditions is required for a precise control of the bright resonance.

In conclusion, we experimentally and theoretically studied the bright resonance Hanle effect on a closed  $F_g=3 \rightarrow F_e=4$  transition for circularly polarized light and a transverse magnetic field. The zero-field-enhanced absorption corresponds to the accumulation, via optical pumping, of the atomic population in ground states maximally coupled to the excited state. The application of a magnetic field redistributes the population among the ground-state sublevels, and results in a decrease of the fluorescence intensity. The efficient production of low-frequency coherences realized in the present Hanle effect configuration produces a strong dependence on the ground-state relaxation processes and on the spurious magnetic fields, to be explored under highly controlled experimental conditions.

The experimental investigations reported here were performed by S.C. while visiting the Dipartimento di Fisica, Università di Pisa, I-56126 Pisa, with the financial support of the NATO-CNR Senior Guest Fellowship Program. F.R. is grateful to G. Grynberg and P. Verkerk for useful discussions.

- 
- [1] *The Hanle Effect and Level-Crossing Spectroscopy*, edited by G. Moruzzi and F. Strumia (Plenum, New York, 1991).
- [2] E. Arimondo, in *Progress in Optics*, edited by E. Wolf (Elsevier, Amsterdam, 1996), Vol. 35, pp. 257–354.
- [3] S. Harris, *Phys. Today* **50**, 36 (1997).
- [4] M. O. Scully and M. S. Zubairy, *Quantum Optics* (Cambridge University Press, Cambridge, 1997).
- [5] J. Dalibard and C. Cohen-Tannoudji, *J. Opt. Soc. Am. B* **6**, 2023 (1989).
- [6] C. Cohen-Tannoudji, in *Fundamental Systems in Quantum Optics*, edited by J. Dalibard, J. M. Raimond, and J. Zinn-Justin (Elsevier, Amsterdam, 1991).
- [7] A. Aspect, E. Arimondo, R. Kaiser, N. Vansteenkiste, and C. Cohen-Tannoudji, *Phys. Rev. Lett.* **61**, 826 (1988).
- [8] A.M. Akulshin, S. Barreiro, and A. Lezama, *Phys. Rev. A* **57**, 2996 (1998); A. Lezama, S. Barreiro, and A.M. Akulshin, *ibid.* **59**, 4732 (1999); A.M. Akulshin, S. Barreiro, and A. Lezama, *Phys. Rev. Lett.* **83**, 4277 (1999).
- [9] Q. Long, S. Zhou, S. Zhou, and Y. Wang, *Phys. Rev. A* **62**, 023406 (2000).
- [10] F. Renzoni, W. Maichen, L. Windholz, and E. Arimondo, *Phys. Rev. A* **55**, 3710 (1997).
- [11] Y. Dancheva, G. Alzetta, S. Cartaleva, M. Taslakov, and Ch. Andreeva, *Opt. Commun.* **178**, 103 (2000).
- [12] F. Renzoni, C. Zimmermann, P. Verkerk, and E. Arimondo, *J. Opt. B: Quantum Semiclassical Opt.* **3**, S7 (2001).
- [13] H.Y. Ling, Y.-Q. Li, and M. Xiao, *Phys. Rev. A* **53**, 1014 (1996).
- [14] J. Sagle, R.K. Namioka, and J. Huennekens, *J. Phys. B* **29**, 2629 (1996), and references therein.